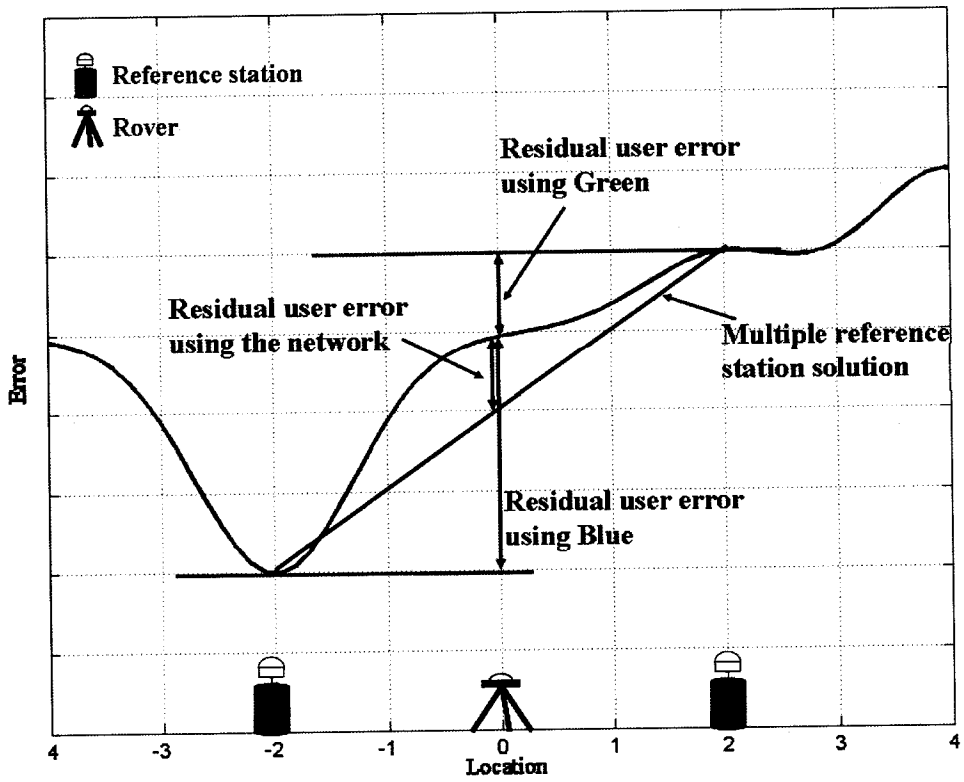

Figure 14: Example of the Measurement Error of One Satellite Across a Region (red line) (This error is measured at two locations indicated by the green and blue reference stations.)

Although there may be times when one reference station's solution is better than the network solution, the network solution is generally more likely to accurately represent the errors over the region because of the additional information gained from combining the data from all reference stations. Figure 15 and Figure 16 (produced by Leica GNSS QC Software) show comparisons of the residual dispersive and non-dispersive errors experienced by a user for both the single reference station and network reference station methods using real data. In all cases, being close to a reference station provides the best solution. The advantage of the multiple reference station model is seen between reference stations outside of the region where typical single reference station RTK processing would be acceptable.

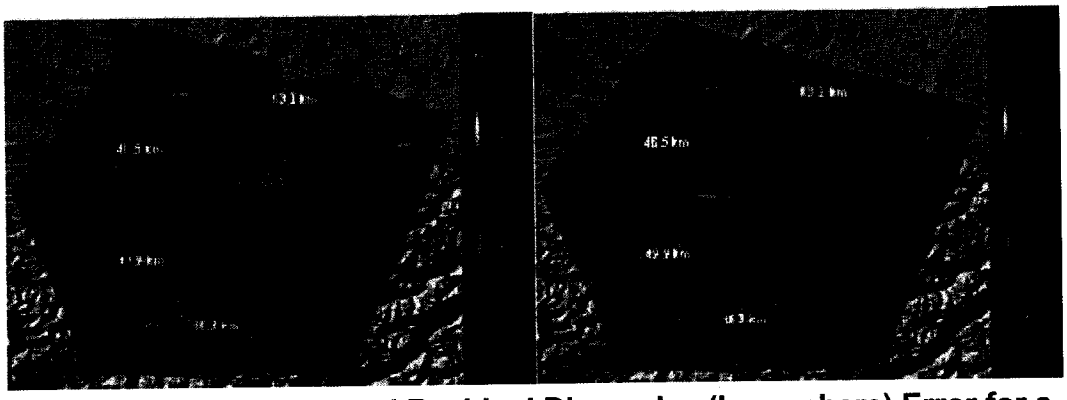

Figure 15: The Estimated Residual Dispersive (Ionosphere) Error for a Single Reference Station User (Left) and a Network Reference Station User (Right)

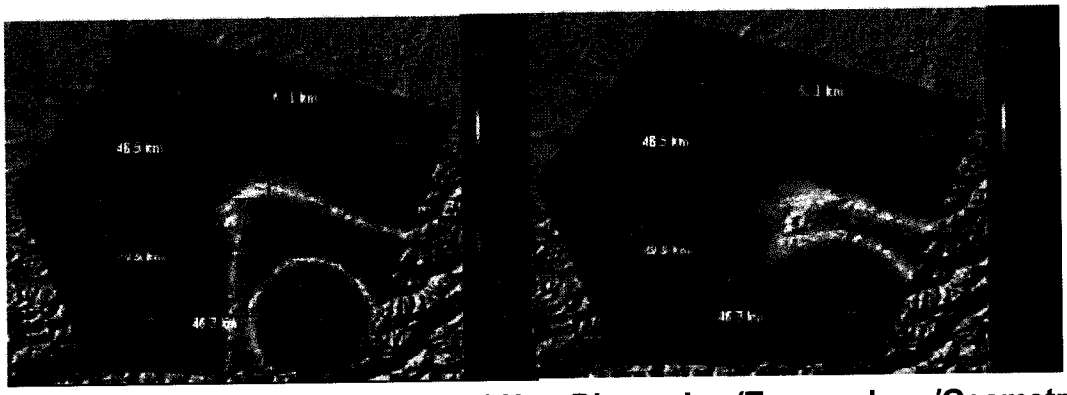

Figure 16: The Estimated Residual Non-Dispersive (Troposphere/Geometry) Error for a Single Reference Station User (Left) and a Network Reference Station User (Right)

In practice, combining the data from multiple reference stations to provide an integrated solution is more complex than the image shown in Figure 14. The following steps must be taken to create the network error model and use it effectively in the user receiver:

1. Accurately measure the relative measurement errors between the reference stations. The most accurate GNSS measurements are phase measurements; however, to use these measurements the carrier phase ambiguities must be precisely estimated and fixed to their correct integer values. To use the integer ambiguities, the double differenced form of the measurements must be used. The double differenced measurement estimates must then be undifferenced for the later steps. This adds significant complexity to the multiple reference station processing.
2. Interpolate the relative measurement errors between the stations to the location of the user.
3. Convert this information to a receiver-acceptable format. There are currently four acceptable options for transmitting network corrections:

a. Master-auxiliary corrections. These corrections contain the absolute errors for one master reference station and the relative errors for all other auxiliary reference stations. For this format, interpolation from step two is performed by the user.
b. Flächen Korrektur Parameter (FKP), or area correction parameters in English. These corrections contain the absolute errors for one master station and the parameters of a regional plane model. In this case interpolation from step two is performed by the user.
c. Single reference station corrections. The single reference station corrections are the absolute corrections for one station combined with the relative predicted errors between that master station and the user. This format option allows for users whose receivers are older and do not support the recently developed network correction formats.
d. Virtual reference station (VRS). VRS corrections are the single reference station corrections (described above) that have been mathematically translated to a virtual geographic location that is closer to the user's location. This location change moves the reference station to a distance that is more representative for the new level of measurement error after applying the network error model.

4. Use the received corrections to calculate the position of the network user.

The main advantage of a multiple-reference station RTK is the improved user performance. However, the improvement in performance can also be analyzed in an opposite manner; namely, as a way to increase the spacing between reference stations while still achieving the same level of performance. The performance improvement is dependent on many factors, including the variability of the measurement errors in the region and the ability to successfully resolve network ambiguities.

A multiple-reference station RTK is more robust against station outages since a network solution can still be calculated even if individual reference station data is missing. However, due to the current trend of sparse network station spacing, the absence of any individual reference station would likely cause pockets within the network with less than desirable performance. The network, even under these conditions, is still more likely to provide a solution better than from a single-reference station.

This improvement comes at a cost of increased complexity and infrastructure. The data from all of the network reference stations must be collected in a central location for processing and then redistributed to network users. The cost of maintaining a processing centre and data communication lines for each reference station may be significant depending on the number of reference stations and the country and region of the network.

6 Review of Integration of GNSS with Inertial Navigation

This section discusses the motivation, methods and results of integrating GNSS with inertial sensors.

6.1 Introduction and Motivation

The overall motivation for integrating GNSS and inertial navigation system (INS) data is to provide a better navigation solution relative to either system alone. To this end, the key characteristics of GNSS and INS are summarized in Table 3 (e.g., Skaloud 1999).

Table 3: Key Characteristics of GNSS and INS

Characteristic	GNSS	INS
Position/Velocity Accuracy	Nearly uniform at all frequencies with higher accuracy at low-frequencies (long-term)	High accuracy at high-frequencies (short-term); errors degrade as a function of time
Attitude	Limited accuracy and requires special equipment setup	Provided as a natural byproduct with high accuracy in the short-term
Measurement Rate	Generally ≤10-20 Hz	Generally ≥50 Hz
Autonomy	Completely reliant on signals from satellites	Self-contained sensors; fully-autonomous
Availability	Function of satellite visibility; may have temporary outages	Fully available (with degrading accuracy)
Susceptibility to Interference	Susceptible to interference	Not susceptible to interference
Gravity	Not affected by gravity	Affected by gravity

A review of Table 3 shows that GNSS and INS are highly complementary, thus making them well suited to integration with each other. Effectively, the GNSS data, when available, is used to "calibrate" the INS errors, thus allowing the INS to provide accurate navigation information when GNSS is temporarily unavailable. This has been widely recognized for many years (as reflected by the many citations provided in this section) and has thus been the focus of ongoing research to improve various aspects of navigation. The benefits of GNSS/INS integration, relative to either system alone, can be summarized as (Hartman 1988; Greenspan 1994):

- Full position, velocity, and attitude solution
- Improved accuracy and availability

- Smoother trajectories
- Greater integrity
- Reduced susceptibility to jamming and interference

Furthermore, for high accuracy applications, GNSS/INS integration can yield improved ambiguity resolution performance (Skaloud 1999; Scherzinger 2000; Scherzinger 2001; Scherzinger 2002; Petovello 2003b; Petovello et al 2003; Scherzinger 2006) and/or help to detect and correct cycle slips (Cannon 1991; Schwarz et al 1994a; Sun et al 1994; Petovello 2003b).

The following sub-sections provide a brief overview of the inertial methodology as well as the performance of various systems quoted in the literature.

6.2 Methodology

The key to understanding inertial-based navigation requires a review of the relevant methodology. This section briefly presents the key aspects of inertial navigation including the sensors involved, the error characteristics, and the methods for integrating with GNSS data. Much of the methodology is provided without mathematical derivation in order to emphasize key points, and readers are referred to the cited material for more information.

6.2.1 Inertial Navigation Basics

The fundamental sensors involved with inertial navigation are the gyroscope and accelerometer. These sensors are discussed in more detail in the sub-sections below, followed by a short discussion of what comprises an INS.

6.2.1.1 Gyroscopes

It is noted that the term "gyroscope," or simply "gyro," is actually a misnomer in many instances, because many current sensors do not use spinning masses (from which the name gyroscope originates). A more accurate term would be "angular rate sensor." Nevertheless, the term "gyro" is used extensively in the literature and has thus been adopted here as well. To this end, a gyro measures the angular rate about its sensitive axis. Several types of gyros are available including, but not necessarily limited to, mechanical gyros, rate gyros, vibrating gyros, optical gyros, and cryogenic gyros (e.g., Titterton and Weston 1997; Jekeli 2000; Grewal et al 2001). Depending on the type of sensor, the errors sources may include time-varying biases, scale factors, misalignments, temperature sensitivity, magnetic sensitivities, and noise (ibid.).

6.2.1.2 Accelerometers

Counter-intuitively, accelerometers do not directly measure acceleration, but rather *specific force*, which is the vector difference of acceleration and gravitational acceleration (not gravity, which is different). As with gyros, there are several different types of accelerometers including pendulous accelerometers, vibrating accelerometers, force rebalancing accelerometers, and strain sensing accelerometers (e.g., Titterton and Weston 1997; Jekeli 2000; Grewal et al 2001). The associated errors may include time-varying

biases, scale factors, misalignments, temperature sensitivity, anisoelasticity effects, and noise (ibid.).

6.2.1.3 Inertial Measurement Unit (IMU)

The term inertial measurement unit (IMU) generally refers to orthogonal triads of accelerometers and gyros mounted in a single enclosure. It should be clear, therefore, that an IMU only measures specific force and angular rates. In contrast, an INS consists of an IMU as well as the necessary electronics to implement the mechanization equations and error equations presented in Section 6.2.2. Herein, the terms IMU and INS are, therefore, not used interchangeably, although it is warned that this does happen occasionally in the literature.

6.2.1.4 Effect of Sensor Quality

The error sources associated with inertial sensors are characterized by their magnitude and variability. The magnitude refers to how large the initial error can be, whereas the variability refers to how quickly and much the error can vary about a mean value. As will be shown later, it is the latter characteristics that are often most important in an integrated GNSS/INS system.

Several different terms have been used to classify the quality of IMUs. Table 4 gives the general classification that will be used in this report. For the time being, however, it is critical to note that lower-cost sensors, especially micro-electro-mechanical system (MEMS) sensors that are used in automotive-grade IMUs, are generally prone to larger and more variable errors. Their reduced size, cost, and power requirements are, therefore, at odds with the development of an accurate navigation system, which would ideally prefer the best quality, and thus most expensive, of sensors.

Table 4: General IMU Classifications (from Petovello 2003b)

Sensor Error	IMU Grade		
	Navigation	**Tactical**	**Automotive**
Gyro Bias (deg/h)	0.005-0.010	1-10	≥100
Accelerometer Bias (m/s^2)	0.050-0.100	2-4	≥12

6.2.2 Equations of Motion and Error Equations

This section presents, without derivation, the equations of motion and the corresponding error equations. The equations follow closely the notation in Jekeli (2000), but similar formulations are presented in, for example, Titterton & Weston (1997) and Grewal, et al. (2001).

6.2.2.1 Equations of Motion

The equations of motions, given by the following three vector differential equations describe the motion and attitude of a body as a function of time:

$$\frac{d\boldsymbol{p}^n}{dt} = \boldsymbol{T}\boldsymbol{v}^n \tag{1}$$

$$\frac{d\boldsymbol{v}^n}{dt} = \boldsymbol{R}_b^n \boldsymbol{f}^b - \left(2\boldsymbol{\omega}_{ie}^n + \boldsymbol{\omega}_{en}^n\right) \times \boldsymbol{v}^n + \boldsymbol{g}^n \tag{2}$$

$$\frac{d\boldsymbol{R}_b^n}{dt} = \boldsymbol{R}_b^n \left(\boldsymbol{\Omega}_{ib}^b - \boldsymbol{\Omega}_{in}^b\right) \tag{3}$$

where $(\bullet)^a$ is a quantity expressed in frame a; $\boldsymbol{p}$ is the position vector; $\boldsymbol{v}$ is the velocity vector; $\boldsymbol{T}$ relates the velocity and (possibly curvilinear) position states; $\boldsymbol{R}_a^b$ is the rotation matrix (direction cosine matrix) from frame a to frame b; $\boldsymbol{f}$ is the specific force vector; $\boldsymbol{\omega}_{ab}^c$ is the angular rate vector of frame b relative to frame a expressed in frame c; $\boldsymbol{g}$ is the gravity (not gravitation) vector, and; $\boldsymbol{\Omega}_{ab}^c$ is the skew-symmetric form of $\boldsymbol{\omega}_{ab}^c$. The subscripts and superscripts refer to the coordinate frame in which the quantity is parameterized. For the purpose of this discussion, the four coordinate frames used are the body (b) frame, the Earth (e) frame, the inertial (i) frame, and the navigation (n) frame (more definitions are available in Jekeli (2000)). In the context of this report, it is assumed that the navigation frame is the local level frame, although this is not required in a general sense. For more details on equations (1) to (3) and/or the relevant coordinate frames, refer to *ibid.*

In equations (2) and (3), the specific force vector, $\boldsymbol{f}^b$, and the measured angular rate vector, $\boldsymbol{\Omega}_{ib}^b$ (in skew-symmetric form), represent the input to the system and the position, velocity, and attitude represent the output. The integration of the differential equations is performed using the *mechanization equations*, which are not discussed here.

6.2.2.2 Error Equations

Although the equations of motion relate the input and outputs of an INS, it is generally more interesting to look at the corresponding error equations. The error equations are obtained by *perturbing*, or *linearizing*, the equations of motion and are given, again without derivation, by:

$$\frac{d\delta\boldsymbol{p}^n}{dt} = \boldsymbol{T}' \cdot \delta\boldsymbol{p}^n + \boldsymbol{T} \cdot \delta\boldsymbol{v}^n \tag{4}$$

$$\frac{d\delta\boldsymbol{v}^n}{dt} = -\left(\boldsymbol{R}_b^n \boldsymbol{f}^b\right) \times \boldsymbol{\varepsilon}^n + \left(2\boldsymbol{\Omega}_{ie}^n + \boldsymbol{\Omega}_{en}^n\right)\delta\boldsymbol{v}^n + \boldsymbol{v}^n \times \left(2\delta\boldsymbol{\omega}_{ie}^n + \delta\boldsymbol{\omega}_{en}^n\right) + \delta\boldsymbol{g}^n + \boldsymbol{R}_b^n \delta\boldsymbol{f}^b \tag{5}$$

$$\frac{d\boldsymbol{\varepsilon}^n}{dt} = \boldsymbol{\omega}_{in}^n \times \boldsymbol{\varepsilon}^n - \delta\boldsymbol{\omega}_{in}^n + \boldsymbol{R}_b^n \delta\boldsymbol{\omega}_{ib}^b \tag{6}$$

where a δ in front of a quantity indicates the error in that quantity, ε is the attitude error, T' relates the position errors to their time derivatives, and the other terms are as described above. Of key importance to this report are the rightmost terms in equations (5) and (6), which contain the accelerometer (δf^b) and gyro ($\delta \omega_{ib}^b$) measurement errors, respectively. As can be seen, these errors directly contribute to the INS velocity and attitude errors respectively (and indirectly to all system errors). Recalling Section 6.2.1.4, it should now be clear why the quality of the inertial sensors is so important in defining the accuracy of the system. In particular, when GNSS data is available, the INS errors (including the IMU errors) can be effectively "calibrated" using the methods described in Section 6.2.3. However, once GNSS data is absent, the error growth of the INS is determined entirely from equations (4) to (6), of which the primary contributors are the sensor errors. As such, the smaller the variability of the errors (relative to when they were last "calibrated" using GNSS data), the better the error behavior will be.

It is also noted that the first term in equation (5) contains the true (but unknown) specific force vector. This means that the level of dynamics (i.e., accelerations) of the vehicle also has an impact on system performance in the absence of GNSS, with larger dynamics resulting in larger error growth.

From the above, to minimize *free-inertial* error of the INS (i.e., the error in the absence of GNSS data), the IMU sensor errors should be small, and the dynamics in the absence of GNSS should be low. Furthermore, the position, velocity, and attitude errors should be small prior to losing GNSS data. The extent to which this is possible will depend on the quality and frequency of the GNSS measurements used in the GNSS/INS integration and on the method of integration, as discussed in Section 6.2.3.

6.2.2.3 *Other Sensor Configurations*

Before continuing, it is also worth noting that considerable research has been directed at using less than a full IMU configuration of accelerometers and gyros (i.e., two triads of each). The motivation for these "reduced IMUs" is to reduce system cost at the expense of not measuring certain vehicle dynamics. However, if certain vehicle motions are not significant (e.g., roll and pitch in automotive applications), then this tradeoff may be justified, as very little information is being omitted.

Although some results obtained using reduced IMUs are discussed in Section 6.3, the details of how to implement these systems are not presented here. Suffice it to say, however, that the equations above can be modified using the appropriate assumptions to yield the relevant equations. For more details on reduced IMU systems refer, for example, to Daum, et al. (1994), Brandt & Gardner (1998), Phuyal (2004), Niu, et al. (2006), Niu, et al. (2007), Syed, et al. (2007), or Sun, et al. (2008).

6.2.3 Integration of GNSS and INS

As mentioned above, the complementary characteristics of GNSS and INS make each well suited for integration. This section discusses the main methods and considerations associated with this integration.

6.2.3.1 Integration Architectures

The concept of GNSS/INS integration is illustrated in Figure 17. As shown, the GNSS receiver and the INS are each capable of generating their own navigation solutions. However, the idea is to combine data from both systems using the "Integration Algorithm" in order to generate a hybrid solution.

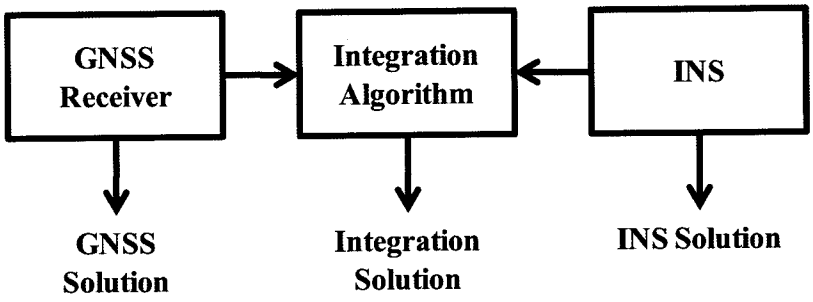

Figure 17: Concept of GNSS/INS Integration

The type of information shared between the GNSS receiver and the INS dictates the type of integration or integration architecture. There are basically three integration architectures, of which the following two are the most common (e.g., Greenspan 1994; Jekeli 2000; Petovello 2003b; Petovello, et al. 2003; Gebre-Egziabher 2007):

- *Loose integration* combines the GNSS and INS data at the position and velocity level. Although relatively simple to implement, this approach tends to exhibit poorer performance when a standalone GNSS solution cannot be computed.
- *Tight integration* combines the GNSS measurements (pseudoranges, carrier phases, and Dopplers) with the INS solution. This approach offers a good tradeoff between complexity and performance. Unlike with loose integration, a tight integration approach still allows the INS to be updated even when a standalone GNSS solution is unavailable due to lack of satellite visibility. As such, the tight integration approach tends to outperform the loose integration approach.

It is noted that some variants on the above terms/definitions are present in the literature. Regardless of the various naming conventions, however, the underlying principles are the same. Of the above two approaches, the tight integration is arguably more popular. As shown in Petovello (2003b) and Petovello, et al. (2003), the differences between the two approaches are negligible as long as GNSS data is available. However, in GNSS-denied areas, the tight integration offers better performance, with larger improvements being realized the longer GNSS data is unavailable.

In addition to the above two approaches, with the recent advent of software-defined receivers (see e.g., Borre et al 2007; Morton 2007; Scott 2007), attention has recently been given to ultra-tight (or deep) integration approaches. In this case, the INS mechanization equations are directly implemented within the tracking loops of the GNSS receiver. The two sensors, therefore, no longer operate independently of each other but rather the GNSS data is used to compensate the IMU errors and the integrated solution is used to help track the GNSS signals, particularly in the presence of high vehicle dynamics and/or interference. Ultra-tight integration strategies are not currently

commercially available and will, therefore, not be discussed further in this report. However, it is noted that ultra-tight integrations have recently been shown to offer superior carrier phase tracking performance than a "standard" GNSS receiver (O'Driscoll, et al. 2008; Petovello, et al. 2008). For more information, refer, for example, to Oppenheim, et al. (1999); Gustafson, et al. (2000); Abbott & Lillo (2003); Gustafson & Dowdle (2003); Kim, et al. (2003); Jovancevic, et al. (2004) ; Soloviev, et al. (2004b; 2004a); Pany, et al, (2005); Kim, et al. (2006); Groves, et al. (2007); Petovello, et al. (2007); O'Driscoll, et al. (2008); and Petovello, et al. (2008).

6.2.3.2 Integration Algorithms

Once the integration architecture is defined, the algorithm used to fuse the GNSS and INS data together must be decided (i.e., the middle box in Figure 17). The Extended Kalman Filter (EKF) is by far the most widely used algorithm used in the literature. The EKF offers an efficient and flexible implementation that suits the GNSS/INS integration problem very well, especially since the filter's basic system model is given by equations (4) to (6) above. Details regarding Kalman filtering are available, for example, in Gelb (1974), Brown & Hwang (1992), Minkler & Minkler (1993), Maybeck 1994, and Grewal & Andrews (2008). For details on how to implement a Kalman filter for GNSS/INS integration, refer to Cannon (Cannon 1991) or Petovello (Petovello 2003b).

Other integration algorithms have also recently been proposed including the Linearized Kalman Filter (LKF) (Nassar, et al. 2005), the Unscented Kalman Filter (UKF) (Nassar, et al. 2005; Yi and Grejner-Brzezinska 2006), the Sigma Point Kalman Filter (SPKF) (Wendel, et al. 2005) and variants of the Particle Filter (PF) (Aggarwal, et al. 2006; Aggarwal 2008), to name a few. With the exception of the LKF, all other methods are based on Bayesian estimation techniques which do not assume Gaussian error distributions. These same methods are also better able to deal with non-linearities in the system model. It is noted, however, that the non-linearities in GNSS/INS systems are generally fairly small, except with very low cost MEMS sensors, and even then usually only during system initialization. As such, these approaches do not always provide significant benefits (Wendel, et al, 2005; Yi and Grejner-Brzezinska 2006). Given the relatively low use rate of these filters in the literature, their limited benefits, and their added complexity (although not necessarily computational burden), these filters are not discussed in detail in this report.

6.2.3.3 System Models

As mentioned earlier, the basic system model for any Kalman filter implementation is given by equations (4) to (6). In addition to this, however, models for the IMU sensor errors, that is, $\delta \boldsymbol{f}^b$ and $\delta \boldsymbol{\omega}_{ib}^b$, need to be developed. Unfortunately, there is no hard and fast rule for this process. Instead, the models will ultimately tradeoff veracity, computational efficiency, observability, and practical performance. Furthermore, all of these will likely be affected by the quality of IMU and the application under consideration. For example, a MEMS-based INS generally performs better if the scale factor and initial bias errors are estimated (Godha and Cannon 2005a). For high dynamics applications, however, scale factor errors may also have to be estimated for higher quality IMUs as well. System developers need to carefully design their filter to optimize performance according to their specific criteria.

6.2.3.4 Extra Aiding Information

Before discussing results presented in the literature, it is worth noting that other sources of aiding can sometimes be incorporated into the system for little or no cost. Three such aiding sources are discussed here. First, a barometer can be used to control the height component of the navigation solution (Lachapelle, et al. 2003), assuming all systematic errors are accounted for (e.g., Garin, et al. 2008). Although this can greatly improve the GNSS navigation solution in the horizontal and vertical directions (Lachapelle, et al. 2003), it does not directly influence the horizontal components of the INS solution (Gebre-Egziabher 2004). However, in an integrated system, the improved GNSS solution has been shown to have a positive effect on the overall system accuracy, especially in the absence of GNSS data (Godha and Cannon 2005a; Godha, et al. 2005), because the improved GNSS solutions are better able to calibrate the INS errors. Second, zero velocity updates (ZUPTs) can be used to effectively provide additional information to the system, assuming the stopping condition can be accurately and reliably identified. Third, non-holonomic constraints (NHCs) assume the vehicle travels along its longitudinal axis only. By enforcing zero accelerations in the lateral and vertical channels, improved performance can be obtained (Godha and Cannon 2005b; Godha and Cannon 2005a; Niu and El-Sheimy 2005; Syed, et al. 2007). Closely related to NHC is the use of an odometer (or wheel speed sensor) to also measure the longitudinal velocity. This approach is well suited to vehicles with anti-lock braking systems.

6.3 Review of Published Results

This section presents a summary of the key results quoted in the literature. Results are presented assuming real-time processing. In other words, the benefits of backward smoothing (Gelb 1974; Brown and Hwang 1992; Minkler and Minkler 1993; Maybeck 1994; Hide, et al. 2006; Grewal and Andrews 2008) or near real-time processing (e.g., Nassar and Schwarz 2001) are not addressed.

Given the breadth of GNSS/INS research, it is impossible to summarize all work in the literature (as an example, a search for "INS" on the U.S. Institute of Navigation (ION) website turned up over 300 papers and a search for "inertial navigation" on the IEEE Explore website turned up over 500 more). Instead, the results presented below are, in the authors' expert opinion, a representative subset of the work that relates (directly or otherwise) to the field of vehicular navigation. Results are categorized as follows, with more attention given to the latter two categories because of their relevance to context of this work:

- Results with navigation-grade IMUs
- Results with tactical-grade IMUs
- Results with automotive-grade IMUs (i.e., MEMS)
- Results with reduced IMUs

All of the main results are presented in tabular form on pages 39 to 45, with additional information provided in the text to highlight key points. Furthermore, as needed, the various sections are augmented with references that are also relevant to this report such as

the effect of height aiding (e.g., from a barometer) or the effect of ZUPTs or other velocity constraints.

Unless otherwise stated, all IMU specifications refer to the turn-on bias stability, not the in-run stability. That said, it should be noted that IMU specifications are *not* guaranteed and differences, in some cases significant, will occur from unit to unit. Some care should, therefore, be taken when interpreting and comparing the results between citations.

6.3.1.1 Results with Navigation-Grade IMU

Results obtained with navigation-grade IMUs are summarized in Table 5. Given the quality of the IMU, the desired accuracy for these studies is at the cm-level. Nevertheless, results give initial impressions regarding the degradation of position accuracy in the absence of GNSS data. In Nassar & Schwarz (2001) different integration algorithms showed a slight improvement in the mean error when using a UKF, but given that the standard deviations of the different solutions are at the 40-55 cm level, these differences are not considered statistically significant.

6.3.1.2 Results with Tactical-Grade IMUs

Table 6 summarizes the results obtained with tactical-grade IMUs. Overall, the results are highly compatible, as should be expected with the relatively good sensors involved.

In Scherzinger (2000) and Petovello, et al. (2003) partial GPS coverage was shown to provide a considerable improvement in positioning accuracy. This illustrates the benefit of the tight integration approach, since in the same environment a loose integration would not be able to compute a GPS-only solution.

In Ford, et al. (2001b), the benefits of ZUPTs are also demonstrated. It is noted, however, that detection of zero velocity conditions is not necessarily trivial; and incorrectly identifying a ZUPT will cause large systematic errors to enter the system.

6.3.1.3 Results with Automotive-Grade IMUs

Results obtained using automotive-grade IMUs are summarized in Table 7. There are three things worth noting. First, the inclusion of a barometer does not significantly improve the overall positioning accuracy (Godha and Cannon 2005b; Godha, et al. 2005; Grejner-Brzezinska, et al. 2006). This is understandable since, in the short term, free-inertial errors are generally larger in the horizontal channel than in the vertical channel. Furthermore, since a barometer has very limited benefit to the horizontal channel in the absence of GNSS data (Gebre-Egziabher 2004), little overall benefit should be expected. Second, NHCs and odometer (or wheel pick-off) data provide an effective means of limiting error growth in vehicular applications (Ford, et al. 2004; Godha and Cannon 2005b; Niu and El-Sheimy 2005). Fortunately, the NHC requires no additional sensors, but can cause problems during turns when the underlying assumptions no longer apply. In this case, the vehicle's side slip angle has to be modeled or calculated (Gao, et al. 2007). Third, compared with the higher grade inertial units, there appears to be a larger difference in positioning performance depending on the integration algorithm used (Nassar, et al. 2005). In particular, the poor results of the LKF are the result of the feed-forward implementation, which, for low-cost IMUs, does not satisfy the inherent assumptions of the system model. That said there does not appear to be a major advantage to using a UKF over and EKF.

In addition to the citations included in Table 7, the following studies are also worth mentioning:

- When GNSS is available, the accuracy of the integrated solutions are commensurate with the quality of GNSS data provided (Wolf, et al. 1997; Farrell, et al. 2000; Yang, et al. 2000). In other words, in ideal GNSS conditions, the inertial sensors provide little, if any, accuracy benefits and serves mainly as an "interpolator" of the GNSS data.
- In Godha & Cannon (2005a), no GPS outages are simulated, but it is shown that estimation of the scale factor errors is important for MEMS-grade sensors, both during turns (even if GPS data is available) and in the absence of GNSS data. For the latter case, inclusion of the scale factor errors provides a 55 percent accuracy improvement over 30 s. Furthermore, when the scale factor estimation and NHC are combined, the positioning results are 80 percent better than when neither is used.
- Bird & Arden (2003) conducted a series of simulations to assess the positioning performance of different combinations of IMU quality (1, 100 and 3600 deg/h gyro) and GPS updates (position and/or velocity updates at 0.1 Hz or 1 Hz). Although a full recap of the results is beyond the scope of this report, the key findings were as follows (their application objective was 1 m position accuracy over 600 s):
  - A high accuracy IMU could meet the system requirements using position and velocity updates at either rate.
  - A medium accuracy IMU could meet the system requirements using position and velocity updates using only 1 Hz update (not with 0.1 Hz updates).
  - A high accuracy IMU with only velocity updates was close to meeting the 1 m requirement.
  - A medium accuracy IMU with low rate (0.1 Hz) position and velocity updates were close to meeting the requirements.

  It is noted, however, that being based on simulations, the above results are likely optimistic. Nevertheless, they give a good idea as to some of the tradeoffs between IMU quality, GPS measurement quality and frequency, and positioning accuracy.

6.3.1.4 Results with Reduced IMUs

Table 8 summarizes the results obtained using reduced IMU configurations. All of the results presented involve low-cost sensors and, given the elimination of some of the IMU sensors, the error growth is more rapid than presented in the previous section. As before, however, the use of the NHC and/or odometer helps to dramatically reduce the positioning errors (Niu, et al. 2006; Syed, et al. 2007).

Table 5: Summary of Results with Navigation-Grade IMUs

Citation	IMU Biases	System Updates	Comments/Notes
Schwarz, et al. (1994b)	Accel: 5 μg (1σ) Gyro: 0.01 deg/h (1σ)	• Real-time kinematic (RTK)	• Free-inertial 3D position error of 10 cm after 30 s without GPS data.
Kumagai, et al. (2000)	Accel: 80 μg (1σ) Gyro: 0.03 deg/h (1σ)	• DGPS	• Free-inertial horizontal position error of approximately 10 m after 3 min without GPS data but with a wheel encoder (odometer).
Nassar & Schwarz (2001)	Accel: 30 μg (1σ) Gyro: 0.0035 deg/hr (1σ)	• DGPS	• Mean 3D position error over 60 s was 0.85 m, 0.75 m and 0.60 m using LKF, EKF, and UKF, respectively.

Table 6: Summary of Results with Tactical-Grade IMUs

Citation	IMU Biases	System Updates	Comments/Notes
Scherzinger (2000)	Accel: 0.5 mg Gyro: 3 deg/h	• RTK GPS	• During full GPS outages, horizontal position error standard deviations were 0.1 m over 10 s, 0.5 m over 30 s, and 1.8 m over 60 s. • With only three GPS satellites visible, the horizontal position error standard deviations were 0.1 m 0.25 m and 0.3 m over 10, 30 and 60 s, respectively.
Scherzinger (2001)	Accel: 1.5 mg Gyro: 3 deg/h	• Dual-frequency RTK • Odometer was also used	• RMS horizontal position errors ranged from 0.1 m over 10 s to 1.4 m over 120 s, and even as high as 6.0 m over 600 s.
Ford, et al. (2001a)	Accel: 1 mg Gyro: 1 deg/h	• GPS RTK	• Approximately 0.2 m RMS position errors (north and east) after 10 s GPS outage, and approximately 10-23 m over a 20 s outage.
Ford, et al. (2001b)	Accel: 1 mg Gyro: 1 deg/h	• GPS RTK	• RMS free-inertial position error with ZUPTs was 0.22 m, 0.29 m, and 0.17 m in the north, east, and vertical directions, respectively after 30 s. After 120 s, the same values were 0.41 m, 0.39 m, and 0.34 m. • Without ZUPTs, the above errors increase to 0.29 m, 0.35 m, and 0.17 m after 30 s, and 0.53 m, 0.49 m, and 0.70 m after 120 s.
Petovello, et al. (2003)	Accel: 1 mg Gyro: 1 deg/h	• GPS RTK	• Using a tight integration during complete GPS outages, the RMS horizontal position errors were 20 cm after 10 s and increased to 2.15 m after 40 s; 3D errors were only slightly worse. • During partial GPS outages (2-3 satellites visible), the RMS 3D position errors were reduced to ≤15 cm after 10 s and 1 m after

Citation	IMU Biases	System Updates	Comments/Notes
			40 s. • The above results are for L1 carrier phase data. Slightly worse performance was obtained when using the wide-lane linear combination. • Using a loose integration architecture, slightly worse results than above were achieved.
Nassar, et al. (2005)	Accel: 1 mg Gyro: 1 deg/h	• DGPS	• Mean 3D position error after 60 s ranged from 1.7-3.0 m, depending on the integration algorithm (LKF was best, then EKF, then UKF).

Table 7: Summary of Results with Automotive-Grade IMUs

Citation	IMU Biases	System Updates	Comments/Notes
Salychev & Voronov (2000)	Accel: <12.5 mg Gyro: <2 deg/s (7200 deg/h)	• Differential GPS and GLONASS	• Free-inertial RMS position errors were 3 m and 10 m over 30 s with constant and high vehicle dynamics, respectively. • Over 20 s, the RMS errors were 10 m and 23 m, respectively.
Ford, et al. (2004)	Accel: 10 mg Gyro: 100 deg/h	• DPGS with carrier smoothing in the position domain	• Free-inertial RMS position errors during 10 s of complete GPS outage were: o 0.48 m, 0.38 m and 0.21 m in the north, east, and vertical directions, respectively. o 0.43 m, 0.35 m, and 0.21 m in the north, east, and vertical directions, respectively, if the IMU misalignments and scale factors were estimated. o Inclusion of wheel pick-off data improves results by an average of 30 percent in each coordinate direction.
Godha & Cannon (2005b)	Accel: 30 mg Gyro: 5400 deg/h	• DGPS in urban canyon	• Horizontal RMS errors in urban canyon were: o INS only: 5.66 m o INS + Height constraint: 4.60 m o INS + NHC: 3.71 m o INS + Height constraint + NHC: 3.37 m
Godha, et al. (2005)	Accel: 30 mg Gyro: 5400 deg/h	• High-sensitivity GPS • Magnetometer (simulated)	• Horizontal RMS errors in urban canyon were: o INS only: 16.9 m o INT + Heading: 14.1 m o INS + Height constraint: 12.2 m • INS + Heading + Height constraint: 7.30 m
Nassar, et al.	Accel: 0.2	• DGPS	• Mean 3D position error after 60 s

Citation	IMU Biases	System Updates	Comments/Notes
(2005)	mg Gyro: 0.01 deg/h		of 3071.2 m, 164.9 m, and 198.5 m using an LKF, EKF, and UKF, respectively.
Niu & El-Sheimy (2005)	Accel: 0.2 mg Gyro: 0.01 deg/s	• GPS RTK	• Mean free-inertial position error after 30 s of 28.3 m with INS alone, 10.9 m with NHC, and 3.3 m with NHC and an odometer.
Mather, et al. (2006)	Accel: N/A Gyro:100 deg/h	• High-sensitivity GPS	• No GPS outages included. • ZUPTs are shown to reset position error to 1 m for static tests, and roughly 20 m for a simulated kinematic test. • Height error with barometer is limited only by the barometer; no impact on horizontal error.
Grejner-Brzezinska, et al. (2006)	Accel: 8.5 mg Gyro: 1 deg/s	• RTK	• Free-inertial position errors in north, east, and vertical directions of: o 66.9 m, 334.6 m, and 72.1 m over 30 s o 2472.7 m, 6542.0 m, and 1331.4 over 120 s • If a calibrated barometer and a compass are added, the results are: o 476.7 m, 93.8 m, and 11.3 m over 30 s • 3038.4 m, 673.3 m, and 4.8 m over 120 s

Table 8: Summary of Results with Reduced IMUs

Citation	IMU Biases	System Updates	Comments/Notes
Daum, et al. (1994)	Accel: 1 mg Gyro: 1 deg/h	• None	• Using 2 accelerometers and 1 gyro, an accuracy of 1-2.2 percent of distance traveled was demonstrated.
Syed, et al. (2007)	Accel: 0.2 mg Gyro: 0.01 deg/h	• GPS positions	• Considered different number of accelerometers (A) and gyros (G) with full outages. Mean errors over 60 s were (without/with NHC): o Full: 238.5 m / 62.8 m o 2G3A: 412.1 m / 96.3 m o 1G3A: 485.9 m / 110.1 m o 1G2A: 485.1 m / 89.9 m o 1G1A: 807.8 m / 439.8 m o 1G0A: 1042.4 m / 447.3 m
Niu, et al. (2006)	Accel: 0.2 mg Gyro: 0.01 deg/h	• SP GPS	• RMS position errors over a 30 s GPS outage were (full IMU/Reduced IMU consisting of 2 accelerometers and 1 gyro): o INS only: 29.8 m / 71.6 m o INS + NHC: 16.9 m / 22.2 m o INS + NHC + odometer: 6.5 m / 9.2 m
Sun, et al. (2008)	Accel: 30 mg Gyro: 5400 deg/h	• SP GPS	• Develops a "terrain predictor" to account of the effect of non-level terrain on systems with 2 or 3 accelerometers and 1 gyro. • Over 30 s GPS outages, the RMS horizontal position errors were (with/without terrain model): o 2A1G: 103 m / 220 m • 3A1G: 103 m / 221 m

7 Impact of Future GNSS and GPS Modernization

GPS modernization was described in Section 3.3 In addition to the new civil signals being deployed on GPS, several other countries and regions are developing their own global satellite navigation systems. Russia has revitalized its GNSS GLONASS constellation with a massive replenishment program. Currently, 18 satellites are operational and a further two are down for maintenance. All of the 18 operational satellites have been launched since 2005 (RSA 2009). The European Union (EU) is continuing to develop is Galileo GNSS, with two validation satellites currently in orbit; and China is developing its own GNSS, named Compass. Each system and its impact will be reviewed below. While each system is slightly different, if and when all of them are fully operational, there will be on the order of 120 navigation satellites in orbit, each broadcasting civil signals on two or three frequencies, compared to the current 49 satellites transmitting civil signals on 1 or 2 frequencies. The major implication of this is that civil users will have roughly 2.5 times as many satellites and 3 times as many signals to use in order to obtain a navigation solution.

7.1 Impact of New GPS Signals

GPS modernization will have a major effect on civil users (McDonald and Hegarty 2000). First, with the addition of L2C, it will become possible for low cost, dual frequency receivers to be deployed where presently dual frequency civil users of GPS are limited to surveying, geodetic, and scientific users with access to expensive codeless and semi-codeless receivers. The availability of this second signal will allow low cost users to form ionosphere-free observation combinations as well as form the wide-lane phase combination which is essential to RTK operation over long baselines. L2C also contains a data bit free pilot channel, which allows for improved signal acquisition in difficult environments including under foliage and indoors. L5, which will be added next, will provide a higher bandwidth and thus higher resolution pseudorange measurement and allow for improved ionosphere estimation and enable the formation of "extra-wide-lane" phase combinations (L2-L5). The combination of the higher accuracy pseudorange and the extra-wide-lane will in principle allow for instantaneous (single-epoch) ambiguity resolution on short baselines where currently the solution must be estimated over several minutes. Several methods to exploit three frequencies for ambiguity resolution have been proposed and developed (Jung, et al. 2000; Teunissen, et al. 2002; Werner and Winkel 2003; Zhang, et al. 2003; Cocard, et al. 2008; O'Keefe, et al. 2009).

7.2 Potential Use of Galileo, GLONASS, and COMPASS

The development of three additional GNSS: GLONASS, Galileo, and Compass will provide users with a GNSS constellation of up to 120 satellites with typical satellite availabilities of 40 to 48 satellites. The additional positioning geometry provided by these satellites will mean significantly lower HDOP values and improved accuracies. Each of these satellites will be transmitting up to three civil signals. There is the potential for more than 100 signals to be available to a typical civil user at any given time compared to the current 10 typically available for a L1 GPS C/A user. The advantages of employing

these signals will have to be carefully weighed against the increased receiver complexity required to acquire and track them.

Of the three GNSS currently in development, Galileo promises to be the easiest to integrate with GPS. Two of the three proposed Galileo frequencies are common with GPS L1 and L5, thus minimizing the required additional antenna and front-end hardware (HW) required. GLONASS is more problematic as it operates using a Frequency Division Multiple Access (FDMA) scheme (Takac 2009). GPS/GLONASS integration is currently used commercially in surveying applications. The main advantage of this integration is in terms of ambiguity resolution time, particularly in partially masked environments.

The effect of GPS and Galileo integration for code-based positioning has been studied by O'Keefe (2001) and many others. The general conclusion of all of these studies is that additional satellites will result in improved dilution of precision and, therefore, improved positioning accuracy.

The effect of GPS/Galileo integration for carrier phase (RTK) positioning has also been studied extensively, mainly in the context of triple-carrier-ambiguity-resolution algorithms (Lachapelle, et al. 2002; Julien, et al. 2003; Leonard, et al. 2003; Julien, et al. 2004; O'Keefe, et al. 2004; Feng and Rizos 2005; Fernández-Plazaola, et al. 2007; Ji, et al. 2007; Cao, et al. 2008b; O'Keefe, et al. 2009). The main conclusion of all of these papers is that the additional signals and satellites provided by using two systems will greatly improve ambiguity resolution time and ambiguity resolution reliability. Particularly the addition of the third frequency which is a feature of both modernized GPS and Galileo will enable almost instantaneous ambiguity resolution due to the presence of a precise pseudorange on the L5 signal and the ability to form an extra-wide-lane phase combination.

Recently, Cao, et al. (2008b) assessed the carrier phase ambiguity resolution performance of various combinations of GPS and Galileo signals. Table 9 shows the time to first fix, percent correct fix, percent incorrect fix, and percent no fix (ambiguity resolution failure) obtained on a simulated 1 km baseline with various combinations of the three common frequencies that will be available on modernized GPS and Galileo (L1, L2, and L5, which are called E1 and E5a in Galileo). In addition to the obvious results that show adding signals and systems leads to improved performance, there are two important results. First, on a short baseline like this, a dual-frequency dual-system receiver will outperform a triple frequency GPS-only receiver in terms of time to first fix (Scenarios D and F in Table 9) though in both cases ambiguity resolution will be almost instantaneous. Secondly, and more importantly for mass market applications, a single frequency dual-system receiver will outperform a dual frequency receiver (Scenarios B and C compared with E). This is very promising for mass market applications since a dual-system GPS/Galileo L1 receiver would require only one antenna and RF-front-end and simply need changes to the signal processing stage of the receiver, yet would perform considerably better than a GPS-alone system provided the baselines are short. The additional frequencies are more valuable on longer baselines where residual ionospheric error begins to become the limiting error source.

Table 9: Comparison of GPS and Galileo Ambiguity Resolution over a 1 KM Baseline (from Cao, et al. 2008b).

(MTTFF, PCF, PIF, and PNF stand for Mean Time to First Fix, Percent Correct Fix, Percent Incorrect Fix, and Percent No Fix, respectively. The measurements column indicates what observables were considered with L1, L2, and L5 representing the three GPS-phase observables and E1 and E5a the two Galileo signals that share carrier frequencies with L1 and L5, respectively.)

Scenario	Measurements	MTTFF	PCF (%)	PIF (%)	PNF (%)
A	L1	63.8	90	8.75	1.25
B	L1, L2	8.1	100	0	0
C	L1, L5	13.1	98.75	1.25	0
D	L1, L2, L5	3.4	100	0	0
E	L1, E1	3.3	98.75	1.25	0
F	L1, E1, L5, E5a	2.0	100	0	0

Very little public information about the Chinese Compass system is presently available. However, some preliminary work has been done to assess the affect of integrating this system with GPS for carrier phase applications. It is expected that the Compass system will be quite similar to the Galileo system, and thus, its usefulness for GPS augmentation will be similar (Cao, et al. 2008a).

7.2.1 Additional GNSS Constellations

GPS positioning performance can be significantly improved with the addition of signals from other GNSS. Presently the only other operational GNSS is the GLONASS system. The design GLONASS constellation consists of 24 satellites in three 64.8 degree inclined orbital planes that broadcast L1 and L2 signals. The number of GLONASS satellites has varied widely over the past 10 years between as few as 8 and as many as 20. The European Union is developing a GNSS called Galileo. Currently only two test satellites are in orbit; however, the planned constellation calls for 30 satellites in three 55 degree inclined planes. China is also developing a GNSS called Compass, very similarly to Galileo, that will also consist of 30 satellites in 3 inclined planes. The orbital characteristics of all four systems are well described in Van Diggelen (2009).

All of these systems propose to broadcast at least one civil signal near the L1 band, meaning that a single frequency receiver, or at least a single RF-front-end receiving signal from a number of systems with similar frequencies, could simultaneously track satellites from four different GNSS. In this situation, two different approaches could be taken. Either independent solutions could be computed from each system and checked against each other, or observations from all of the systems could be combined to estimate one solution. This second approach is particularly useful in urban canyon environments where it is possible that one system alone would not provide enough visible satellites, but two or more systems would. Combining observations from multiple systems requires some care to ensure that each system is operating on the same time scale and coordinate

system, or that intersystem correction values are available. These are planned for the Galileo navigation message but are not currently available in real time for GLONASS.

To demonstrate the effect of adding satellites from additional systems, median and 95th percentile values of HDOP has been computed over part of North America using the as-designed constellations for GPS, Galileo, GLONASS, and Compass. In this simulation, the effect of inter-system clock bias has been neglected and several proposed geostationary satellites in the Compass system have not been considered as well. GPS and GLONASS are assumed to have 24 satellites each, and Galileo and Compass 30 each. Figure 18, Figure 19, Figure 20, and Figure 21 are maps of 95th percentile HDOP for the GPS-only case and with the sequential addition of Galileo, GLONASS, and Compass, respectively. With only one GNSS, 5 percent of the time HDOP over North America would exceed 5, a relatively poor value, when a 20 degree elevation mask is used. The addition of a second GNSS reduces this value to around two for most of the continent, while the addition of a third and fourth GNSS further reduces the 95th percentile HDOP values to on the order of 1.5 and less than 1, respectively.

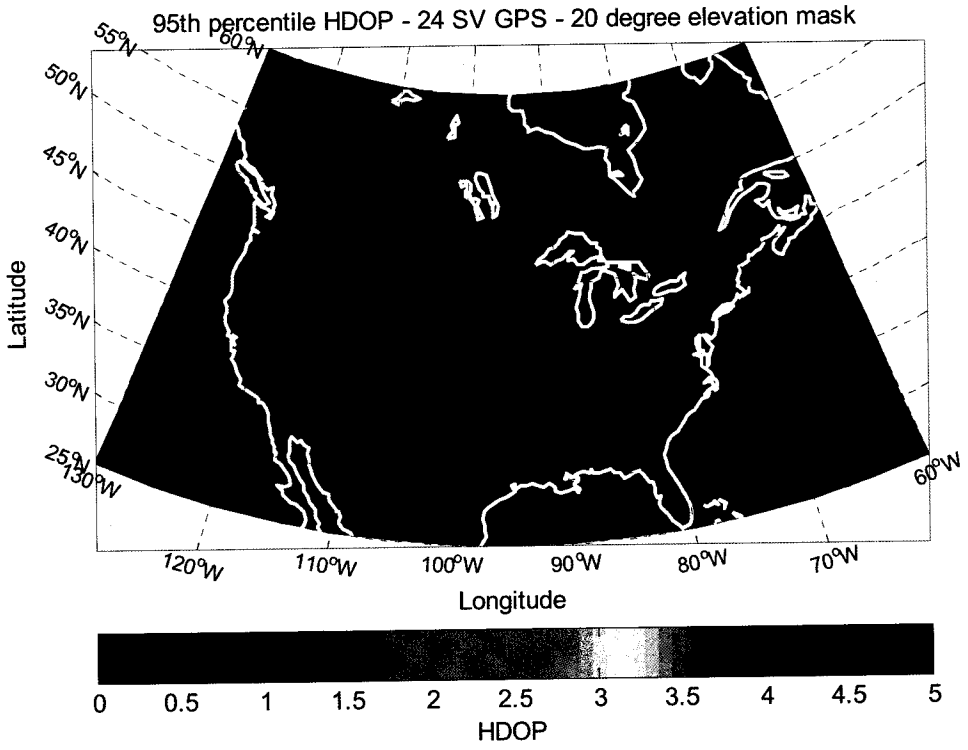

Figure 18: 95th Percentile HDOP Using a 24-Satellite GPS Constellation and a 20-Degree Elevation Mask

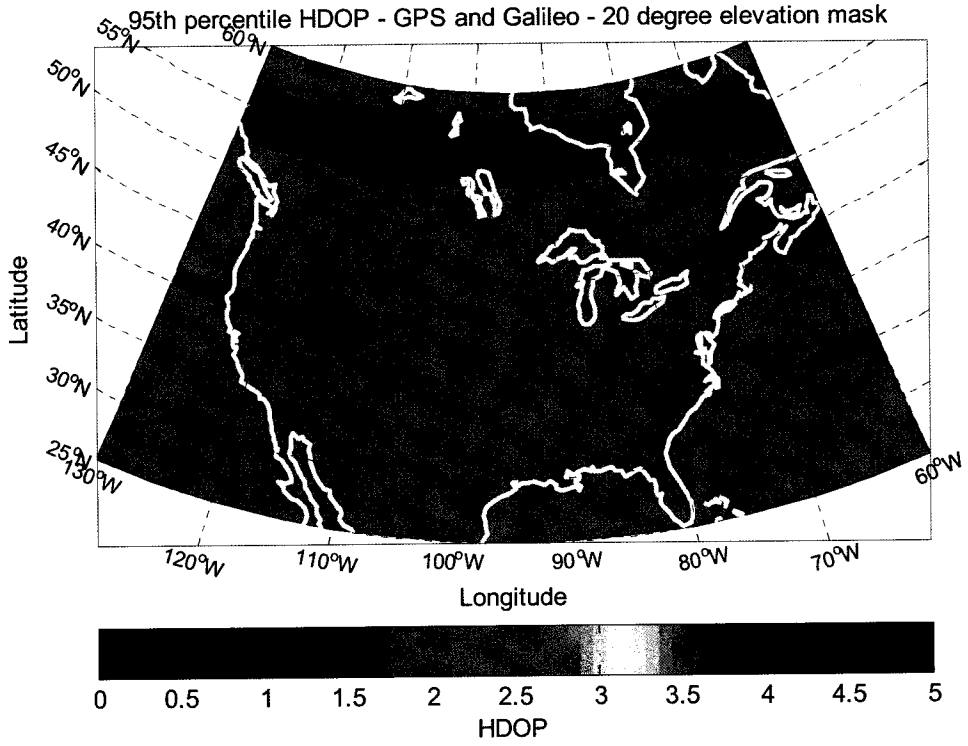

Figure 19: 95th Percentile HDOP Using a 24-Satellite GPS constellation in Conjunction with a 30-Satellite Galileo Constellation and a 20-Degree Elevation Mask

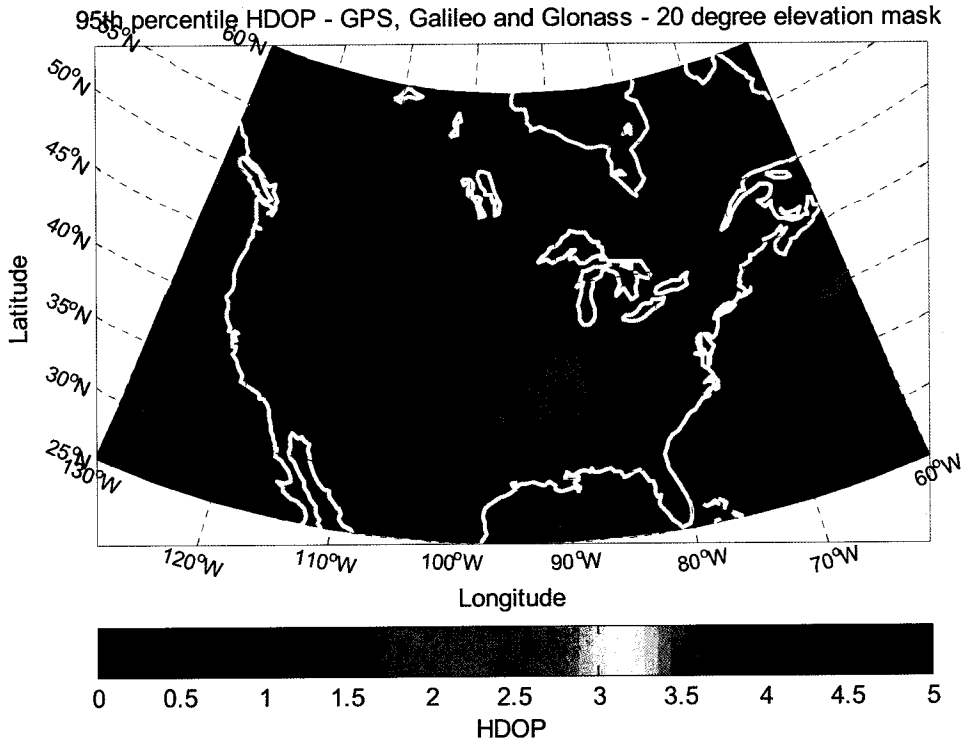

Figure 20: 95th Percentile HDOP Using GPS, Galileo, and GLONASS with a 20-Degree Elevation Mask

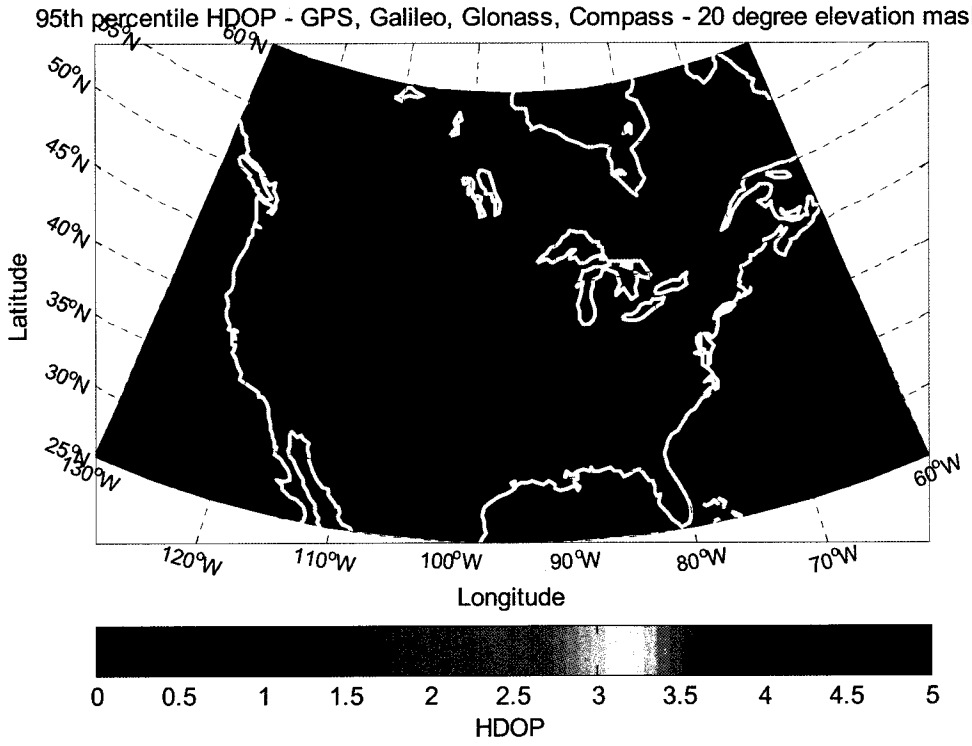

Figure 21: 95th Percentile HDOP Using GPS, Galileo, GLONASS, and Compass with a 20-Degree Elevation Mask

With a 24 satellite GPS and a 20-degree elevation mask, the typical satellite availability ranges between 5 and 8 satellites. Compare this to the 4 GNSS case where between 23 and 27 satellites are in view at all times.

8 References

[1] Abbott, A. S. & W. E. Lillo (2003) Global Positioning Systems and Inertial Measuring Unit Ultratight Coupling Method. United States, The Aerospace Corporation: 22.

[2] Aggarwal, P. (2008) Hybrid Extended Particle Filter (HEPF) for INS/GPS Integrated System. ION GNSS 2008, Savannah, GA, Institute of Navigation: 1600-1609.

[3] Aggarwal, P., D. Gu & N. El-Sheimy (2006) Adaptive Particle Filter for INS/GPS Integration. ION GNSS 2006, Fort Worth, TX, Institute of Navigation: 1606-1613.

[4] Alves (2005) *Development of Two Novel Carrier Phase-Based Methods for Multiple Reference Station Positioning*, PhD Thesis, Department of Geomatics Engineering, University of Calgary, Calgary

[5] Bird, J. & D. Arden (2003) Simulation of Updating Requirements for MEMS-based Inertial Navigation. CASI 14th Symposium on Navigation, Montreal, QC, Canadian Aeronautics and Space Institute.

[6] Borre, K., D. Akos, N. Bertelsen, P. Rinder & S. H. Jenson (2007) *A Software-Defined GPS and Galileo Receiver, A Single-Frequency Approach*, Birkhäuser, Boston.

[7] Brandt, A. & J. F. Gardner (1998) Constrained Navigation Algorithms for Strapdown Inertial Navigation Systems with Reduced Set of Sensors. IEEE American Control Conference, Philadelphia, PA, IEEE: 1848-1852.

[8] Brown, R. G. & P. Y. C. Hwang (1992) *Introduction to Random Signals and Applied Kalman Filtering*, John Wiley & Sons, Inc.

[9] Cannon, M. E. (1991) *Airborne GPS/INS with an Application to Aerotriangulation*, Ph.D. Thesis, Geomatics Engineering, University of Calgary, Calgary

[10] Cao, W., K. O'Keefe & M. E. Cannon (2008a) Evaluation of Compass Ambiguity Resolution Performance Using Geometric-Based Techniques with Comparison to GPS and Galileo. Proceedings of ION GNSS 2008, The Satellite Division of the Institute of Navigation 21th International Technical Meeting, September 16-19, Savannah, GA: 1688-1697.

[11] Cao, W., K. O'Keefe & M. E. Cannon (2008b) Performance Evaluation of Combined GPS/Galileo Multi-frequency RTK Positioning Using Partial Ambiguity Fixing. Proceedings of ION GNSS 2008, The Satellite Division of the Institute of Navigation 21th International Technical Meeting, September 16-19, Savannah, GA: 2841-2849.

[12] Chen, D. & G. Lachapelle (1995) "A Comparison of the FASF and Least-Squares Search Algorithms for Ambiguity Resolution On The Fly." Navigation 42(2): 371-390.

[13] Cocard, M., S. Bourgon, O. Kamali & P. Collins (2008) "A Systematic Investigation of Optimal Carrier-phase Combinations for Modernized Triple-frequency GPS." Journal of Geodesy 82(9): 555-564.

[14] Daum, P., J. Beyer & T. F. W. Kohler (1994) Aided Inertial LAnd NAvigation System (ILANA) with a Minimum Set of Inertial Sensors. IEEE-IEE Vehicle Navigation & Information Systems Conference, IEEE: 284-291.

[15] de Jong, C. D., G. Lachapelle, S. Skone & I. A. Elema (2002) *Hydrography*, Delft University Press, Delft, The Netherlands.

[16] de Jonge, P. & C. C. J. M. Tiberius (1996) The LAMBDA method for integer ambiguity estimation: implementation aspects. Publications of the Delft Geodetic Computing Centre.

[17] DOD (1995) Global Positioning System Standard Positioning Service Signal Specification, 2nd Edition, Department of Defense.

[18] DOD (2008) Global Positioning System Standard Positioning Service Performance Standard. U. Department of Defense, Assistant Secretary of Defense for Command, Control, Communications, and Intelligence.

[19] Erickson, C. (1992) *Investigations of C/A Code and Carrier Measurements and Techniques for Rapid Static GPS Surveys*, MSc Thesis, Geomatics Engineering, University of Calgary, Calgary

[20] FAA (2004) Wide-Area Augmentation System Performance Analysis Report, Report 11. F. A. Administration, NSTB/WAAS T&E Team.

[21] FAA. (2007) "Wide Area Augmentation System WAAS, Fact Sheet."

[22] Farrell, J. A., D. Givargis & M. J. Barth (2000) "Real-Time Differential Carrier Phase GPS-Aided INS." IEEE Transactions on Control Systems Technology 8(4): 709-721.

[23] Feng, Y. & C. Rizos (2005) Three Carrier Approaches for Future Global, Regional and Local GNSS Positioning Services: Concepts and Performance Perspectives. Proceedings of ION GNSS 2005 18th International Technical Meeting of the Satellite Division of the Institute of Navigation Long Beach, CA: 2277 - 2287.

[24] Fernández-Plazaola, U., T. M. Martín-Guerrero & J. T. Entrambasaguas-Muñoz (2007) "A New Method for Three-carrier GNSS Ambiguity Resolution." GPS Solutions.

[25] Ford, T., J. Neumann & M. Bobye (2001a) OEM4 Inertial: An Inertial/GPS Navigation System on the OEM4 Receiver. International Symposium on Kinematic Systems in Geodesy, Geomatics and Navigation (KIS 2001), Banff, AB, Department of Geomatics Engineering, University of Calgary: 150-168.

[26] Ford, T., J. Hamilton, M. Bobye & L. Day (2004) GPS/MEMS Inertial Integration Methodology and Results. ION GNSS 2004, Long Beach, CA, Institute of Navigation: 1587-1597.

[27] Ford, T., J. Neumann, P. Fenton, M. Bobye & J. Hamilton (2001b) OEM4 Inertial: A Tightly Integrated Decentralized Inertial/GPS Navigation System. ION GPS 2001, Salt Lake City, UT, Institute of Navigation: 3153-3163.

[28] GAO (2009) Significant Challenges in Sustaining and Upgrading Widely Used Capabilities, Report to the Subcommittee on National Security and Foreign Affairs, Committee on Oversight and Government Reform, House of Representatives.

[29] Gao, J., M. G. Petovello & M. E. Cannon (2007) "GPS/Low-Cost IMU/Onboard Vehicle Sensors Integrated Land Vehicle Positioning System." EURASIP Journal on Embedded Systems 2007(Article ID 62616).

[30] Garin, L., S. Venkatraman, P. Gupta, B. J. Kokes & T. A. Smith (2008) Enhancing Altitude Accuracy in Automotive Navigation using MEMS Barometric Sensor with GPS. ION NTM 2008, San Diego, CA, Institute of Navigation: 670-679.

[31] Gebre-Egziabher, D. (2004) *Design and Performance Analysis of a Low-Cost Aided Dead Reckoning Navigator*, PhD Thesis, Stanford University

[32] Gebre-Egziabher, D. (2007) What is the Difference Between 'loose', 'tight', 'ultra-tight' and 'deep' integration strategies for INS and GNSS? Inside GNSS. 2: 28-33.

[33] Gelb, A., Ed. (1974) Applied Optimal Estimation. Cambridge, Massachusetts, The MIT Press.

[34] Godha, S. & M. E. Cannon (2005a) Integration of DGPS with a Low Cost MEMS-Based Inertial Measurement Unit (IMU) for Land Vehicle Navigation Application. ION GNSS 2005, Long Beach, CA, Institute of Navigation: 333-345.

[35] Godha, S. & M. E. Cannon (2005b) Development of a DGPS/MEMS IMU Integrated System for Navigation in Urban Canyon Conditions. GNSS-05, Hong Kong.

[36] Godha, S., M. G. Petovello & G. Lachapelle (2005) Performance Analysis of MEMS IMU/HSGPS/Magnetic Sensor Integrated System in Urban Canyons. ION GNSS 2005, Long Beach, CA, Institute of Navigation: 1977-1990.

[37] Greenspan, R. L. (1994) GPS and Inertial Navigation. Global Positioning System: Theory and Applications. B. W. Parkinson and J. J. Spilker, Jr., American Institute of Aeronautics and Astronautics, Inc. II: 187-220.

[38] Grejner-Brzezinska, D., C. K. Toth, Y. Jwa & S. Moafipoor (2006) Seamless and Reliable Personal Navigator. ION NTM 2006, Monterey, CA, Institute of Navigation: 597-603.

[39] Grewal, M. S. & A. P. Andrews (2008) *Kalman Filtering Theory and Practice Using MATLAB®*, John Wiley & Sons, Inc., Hoboken, NJ.

[40] Grewal, M. S., L. R. Weill & A. P. Andrews (2001) *Global Positioning Systems, Inertial Navigations, and Integration*, John Wiley & Sons, Inc.

[41] Groves, P. D., C. J. Mather & A. A. Macaulay (2007) Demonstration of Non-coherent Deep INS/GPS Integration for Optimised Signal-to-noise Performance. ION GNSS 2007, Fort Worth, TX, Institute of Navigation: 2627-2638.

[42] Gustafson, D. & J. Dowdle (2003) Deeply Integrated Code Tracking: Comparative Performance Analysis. ION GPS/GNSS 2003, Portland, OR, Institute of Navigation: 2553-2561.

[43] Gustafson, D., J. Dowdle & K. Flueckiger (2000) A Deeply Integrated Adaptive GPS-Based Navigator with Extended Range Code Tracking. IEEE PLANS, San Diego, CA, IEEE: 118-124.

[44] Hartman, R. G. (1988) "An Integrated GPS/IRS Design Approach." NAVIGATION: Journal of Institute of Navigation 35(1): 121–134.

[45] Hide, C., T. Moore, C. Hill & D. Park (2006) "Low Cost, High Accuracy Positioning In Urban Environments." THE JOURNAL OF NAVIGATION 59(3): 365–379.

[46] Jekeli, C. (2000) *Inertial Navigation Systems with Geodetic Applications*, Walter de Gruyter, Berlin.

[47] Ji, S., W. Chen, C. Zhao, X. Ding & Y. Chen (2007) "Single epoch ambiguity resolution for Galileo with the CAR and LAMBDA methods." GPS Solutions 11(4): 259-268.

[48] Jovancevic, A., A. Brown, S. Ganguly, J. Noronha & B. Sirpatil (2004) Ultra Tight Coupling Implementation Using Real Time Software Receiver. ION GNSS 2004, Long Beach, CA, Institute of Navigation: 1575-1586.

[49] Julien, O., P. Alves, M. E. Cannon & W. Zhang (2003) A Tightly Coupled GPS/GALILEO Combination for Improved Ambiguity Resolution. Proceedings of the European Navigation Conference ENC-GNSS 2003, 22-25 April, Graz, Austria: CD Rom - 14 Pages.

[50] Julien, O., P. Alves, M. E. Cannon & G. Lachapelle (2004) Improved Triple-Frequency GPS/GALILEO Carrier Phase Ambiguity Resolution Using a Stochastic Ionosphere Modeling. Proceedings of ION NTM-04, 26-28 January, San Diego, CA: 441 - 452.

[51] Jung, J., P. Enge & B. Pervan (2000) Optimization of Cascade Integer Resolution with Three Civil GPS Frequencies. Proceedings of the 13th International Technical Meeting of the Satellite Division of the Institute of Navigation ION GPS-2000. Salt Lake City, UT, Institute of Navigation: 2191 - 2201.

[52] Kim, H. S., S. C. Bu, G. I. Jee & C. G. Park (2003) An Ultra-Tightly Coupled GPS/INS Integration Using Federated Filtering. ION GPS/GNSS 2003, Portland, OR, Institute of Navigation: 2878-2885.

[53] Kim, J. W., D.-H. Hwang & S. J. Lee (2006) A Deeply Coupled GPS/INS Integrated Kalman Filter Design using Linearized Correlator Output. ION Annual Meeting/IEEE PLANS, San Diego, CA, Institute of Navigation and IEEE: 300-305.

[54] Klobuchar, J., P. Dorherty & M. B. El-Arini (1995) "Potential Ionospheric Limitations to GPS Wide-Area Augmentation System (WAAS)." Navigation 42(2): 353-379.

[55] Kumagai, H., T. Kindo & S. Sugimoto (2000) DGPS/INS/VMS Integration for High Accuracy Land-Vehicle Positioning. ION GPS 2000, Salt Lake City, UT, Institute of Navigation: 1845-1853.

[56] Lachapelle, G., M. E. Cannon, K. O'Keefe & P. Alves (2002) "How will Galileo Improve Positioning Performance?" GPS World 13(9): 38-48.

[57] Lachapelle, G., O. Mezentsev, J. Collin & G. MacGougan (2003) Pedestrian and Vehicular Navigation Under Signal Masking Using Integrated HSGPS and Self Contained Sensor Technologies. World Congress, International Association of Institutes of Navigation, Berlin.

[58] Leick (2004) *GPS Satellite Surveying*, John Wiley and Sons.

[59] Leonard, A., H. Krag, G. Lachapelle, K. O'Keefe, C. Huth & S. C (2003) Impact of GPS and Galileo Orbital Plane Drifts on Interoperability Performance Parameters. Proceedings of GNSS03, Graz, Austria: Session C-2, 11 pages.

[60] Leva, J., M. W. de Haag & K. Van Dyke (1996) Performance of Standalone GPS. Understanding GPS Principles and Applications. E. D. Kaplan. Boston, Artech House.

[61] MacGougan, G. (2003) *High Sensitivity GPS Performance Analysis in Degraded Signal Environments*, MSc Thesis, Department of Geomatics Engineering, University of Calgary, Calgary

[62] Mather, C. J., P. D. Groves & M. R. Carter (2006) A Man Motion Navigation System Using High Sensitivity GPS, MEMS IMU and Auxiliary Sensors. ION GNSS 2006, Fort Worth, TX, Institute of Navigation: 2704-2714.

[63] Maybeck, P. S. (1994) *Stochastic Models, Estimation and Control*, NavtechGPS.

[64] McDonald, K. & C. Hegarty (2000) Post-Modernization GPS Performance Capabililties. ION AM 2000 Proceedings of the Institute of Navigation 56th Annual Meeting, San Diego, California: 242-249.

[65] Minkler, G. & J. Minkler (1993) *Theory and Application of Kalman Filtering*, Magellan Book Company, Palm Bay, FL.

[66] Misra, P. & P. Enge (2001) *Global Positioning System, Signals, Measurements, and Performance*, Ganga-Jamuna Press, Lincoln, Massechusetts.

[67] Morton, J. (2007) "Expert Advice: Software Defines Future." GPS World System Design and Test News.

[68] Nassar, S. & K.-P. Schwarz (2001) Bridging DGPS Outages in Kinematic Applications Using A Simple Algorithm for INS Bias Modeling. International Symposium on Kinematic Systems in Geodesy, Geomatics and Navigation (KIS 2001), Banff, AB, Department of Geomatics Engineering, University of Calgary: 401-408.

[69] Nassar, S., E. W. Shin, X. Niu & N. El-Sheimy (2005) Accurate INS/GPS Positioning with Different Inertial Systems Using Various Algorithms for Bridging GPS Outages. ION GNSS 2005, Long Beach, CA, Institute of Navigation: 1401-1410.

[70] Niu, X. & N. El-Sheimy (2005) The Development of a Low-cost MEMS IMU/GPS Navigation System for Land Vehicles Using Auxiliary Velocity Updates in the Body Frame. ION GNSS 2005, Long Beach, CA, Institute of Navigation: 2003-2012.

[71] Niu, X., S. Nassar, C. Goodall & N. El-Sheimy (2007) "A Universal Approach for Processing any MEMS Inertial Sensor Configuration for Land-Vehicle Navigation." The Journal of Navigation: 233–245.

[72] Niu, X., S. Nassar, Z. Syed, C. Goodall & N. El-Sheimy (2006) The Development of A MEMS-Based Inertial/GPS System for Land-Vehicle Navigation Applications. ION GNSS 2006. Fort Worth, TX, Institute of Navigation: 1516-1525.

[73] O'Driscoll, C., M. G. Petovello & G. Lachapelle (2008) Impact of Extended Coherent Integration Times on Weak Signal RTK in an Ultra-Tight Receiver. NAV08 Conference. London, UK, Royal Institute of Navigation.

[74] O'Keefe, K. (2001) Availability and Reliability Advantages of Galileo/GPS Integration. Proceedings of ION GPS2001, The Satellite Division of the Institute of Navigation 14th International Technical Meeting, Salt Lake City, Utah: 2096-2104.

[75] O'Keefe, K., S. Ryan & G. Lachapelle (2002) "Global Availability and Reliability Assessment of the GPS and Galileo Global Navigation Satellite Systems." Canadian Aeronautics and Space Journal 48(2): 123-132.

[76] O'Keefe, K., O. Julien, M. E. Cannon & G. Lachapelle (2004) Evaluation of the Availability, Accuracy, Reliability and Carrier-Phase Ambiguity Resolution Capabilities of the Galileo GNSS in Conjunction with Modernized GPS. Proceedings of IAC 2004, the 2004 International Astronautical Congress, Vancouver, British Columbia: 12 Pages.

[77] O'Keefe, K., M. Petovello, W. Cao, G. Lachapelle & E. Guyader (2009) "Comparing of Multi-carrier Ambiguity Resolution methods for Geometry-Based GPS and Galileo Low Earth Orbiting Satellite Attitude Determination." International Journal of Navigation and Observation 2009(Article ID 592073): 15 pages.

[78] Olynik, M. (2002) *Temporal Characteristics of GPS Error Sources and Their Impact on Relative Positioning*, MSc Thesis, Geomatics Engineering, University of Calgary, Calgary

[79] Oppenheim, A. V., R. W. Schafer & J. R. Buck (1999) *Discrete-Time Signal Processing*, Prentice Hall, Upper Saddle River, NJ.

[80] Pany, T., R. Kaniuth & B. Eissfeller (2005) Deep Integration of Navigation Solution and Signal Processing. ION GNSS 2005, Long Beach, CA, Institute of Navigation: 1095-1102.

[81] Parkinson, B. W. (1996) Introduction and Heritage of NAVSTAR, the Global Positioning System. Global Positioning System: Theory And Applications. B. W. Parkinson and J. J. Spilker, Jr. Washington, American Institute of Aeronautics and Astronautics. 1.

[82] Parkinson, B. W. & J. J. Spilker, Jr., Eds. (1996) Global Positioning System: Theory and Applications. Profess in Astronautics and Aeronautics. Washington, American Institute of Aeronautics and Astronautics.

[83] Petovello, M. (2003a) *Real-Time Integration of a Tactical-Grade IMU and GPS for High-Accuracy Positioning and Navigation*, PhD Thesis, Department of Geomatics Engineering, University of Calgary, Calgary

[84] Petovello, M. G. (2003b) *Real-Time Integration of a Tactical-Grade IMU and GPS for High-Accuracy Positioning and Navigation*, Ph.D. Thesis, Geomatics Engineering, University of Calgary, Calgary

[85] Petovello, M. G., M. E. Cannon & G. Lachapelle (2003) "Benefits of Using a Tactical Grade INS for High Accuracy Positioning." NAVIGATION: Journal of Institute of Navigation 51(1): 1-12.

[86] Petovello, M. G., C. O'Driscoll & G. Lachapelle (2007) Ultra-Tight GPS/INS for Carrier Phase Positioning In Weak-Signal Environments. NATO RTO SET-104 Symposium on Military Capabilities Enabled by Advances in Navigation Sensors. Antalya, Turkey, NATO: 18.

[87] Petovello, M. G., C. O'Driscoll & G. Lachapelle (2008) Weak Signal Carrier Tracking Using Extended Coherent Integration with an Ultra-Tight GNSS/IMU Receiver. European Navigation Conference. Toulouse, France: 11.

[88] Phuyal, B. (2004) An Experiment for a 2-D and 3-D GPS/INS Configuration for Land Vehicle Applications. IEEE PLANS 2004, IEEE: 148-152.

[89] Raquet, J. (1998) *Development of a Method for Kinematic GPS Carrier-Phase Ambiguity Resolution Using Multiple Reference Receiver*, PhD Thesis, Department of Geomatics Engineering, University of Calgary, Calgary

[90] Ray, J. (2000) *Mitigation of GPS Code and Carrier Phase Multipath Effects Using a Multi-Antenna System*, PhD Thesis, Department of Geomatics Engineering, University of Calgary, Calgary

[91] RSA. (2009) "Russian Space Agency Information Analytical Centre - GLONASS Status." Retrieved June 24, 2009.

[92] Salychev, O. S. & V. V. Voronov (2000) Low Cost INS/GPS Integration: Concepts and Testing. ION NTM 2000, Anaheim, CA, Institute of Navigation: 98-205.

[93] Scherzinger, B. M. (2000) Precise Robust Positioning with Inertial/GPS RTK. ION GPS 2000, Salt Lake City, UT, Institute of Navigation: 155–162.

[94] Scherzinger, B. M. (2001) Robust Inertially Aided RTK Position Measurement. International Symposium on Kinematic Systems in Geodesy, Geomatics and Navigation (KIS 2001), Banff, AB, Department of Geomatics Engineering, University of Calgary: 265–272.

[95] Scherzinger, B. M. (2002) Robust Positioning with Single Frequency Inertially Aided RTK. ION GPS 2002, Portland, OR, Institute of Navigation: 911–917.

[96] Scherzinger, B. M. (2006) "Precise Robust Positioning with Inertially Aided RTK." NAVIGATION: Journal of Institute of Navigation 53(2): 73-83.

[97] Schleppe, J. (2006) The Suitability of the u-blox LEA-4T for Heading Determination. PLAN Group Internal Document. Calgary, University of Calgary.

[98] Schwarz, K.-P., N. El-Sheimy & Z. Liu (1994a) Fixing GPS Cycle Slips by GPS/INS - Methods and Experience. International Symposium on Kinematic Systems in Geodesy, Geomatics and Navigation (KIS 1994), Banff, AB, Department of Geomatics Engineering, University of Calgary: 265–275.

[99] Schwarz, K.-P., N. El-Sheimy & Z. Liu (1994b) Fixing GPS Cycle Slips by INS/GPS - Methods and Experiences. International Symposium on Kinematic Systems in Geodesy, Geomatics and Navigation (KIS 1994), Banff, AB, Department of Geomatics Engineering, University of Calgary: 265-275.

[100] Scott, L. (2007) "Directions 2008: Software-Defined Radio Role to Grow." GPS World System Design and Test News, Retrieved January 7, 2008.

[101] Shrestha (2003) *Investigations into the Estimation of Tropospheric Delay and Wet Refractivity Using GPS Measurements*, MSc Thesis, Department of Geomatics Engineering, University of Calgary, Calgary

[102] Skaloud, J. (1999) *Optimizing Georeferencing of Airborne Survey Systems by INS/DGPS*, Ph.D. Thesis, Geomatics Engineering, University of Calgary, Calgary

[103] Soloviev, A., F. van Grass & S. Gunawardena (2004a) Implementation of Deeply Integrated GPS/Low-Cost IMU for Reacquisition and Tracking of Low CNR GPS Signals. ION National Technical Meeting, San Diego, CA, Institute of Navigation: 923-935.

[104] Soloviev, A., S. Gunawardena & F. Van Grass (2004b) Deeply Integrated GPS/Low-Cost IMU for Low CNR Signal Processing: Flight Test Results and Real Time Implementation. ION GNSS 2004, Long Beach, CA, Institute of Navigation: 1598-1608.

[105] Spilker, Jr., J. J. (1996a) Satellite Constellation and Geometric Dilution of Precision. Global Positioning System: Theory And Applications. B. W. Parkinson

and J. J. Spilker, Jr. Washington, American Insistute of Aeronautics and Astronautics. 1.

[106] Spilker, Jr., J. J. (1996b) GPS Signal Structure and Theoretical Performance. Global Positioning System: Theory And Applications. B. W. Parkinson and J. J. Spilker, Jr. Washington, American Insistute of Aeronautics and Astronautics. 1.

[107] Sun, D., M. G. Petovello & M. E. Cannon (2008) "GPS/Reduced IMU with a Local Terrain Predictor in Land Vehicle Navigation." International Journal of Navigation and Observation 2008.

[108] Sun, H., M. E. Cannon, T. E. Owen & M. A. Meindl (1994) An Investigation of Airborne GPS/INS for High Accuracy Position and Velocity Determination. ION NTM 2004, Institute of Navigation: 801–809.

[109] Syed, Z., P. Aggarwal, X. Niu & N. El-Sheimy (2007) Economical and Robust Inertial Sensor Configuration for a Portable Navigation System. ION GNSS 2007, Fort Worth, TX, Institute of Navigation: 2129-2135.

[110] Takac, F. (2009) GLONASS interfrequency-biases and ambiguity resolution. Inside GNSS. March/April: 24-28.

[111] Teunissen, P., P. Joosten & C. Tiberius (2002) A Comparison of TCAR, CIR and LAMBDA GNSS Ambiguity Resolution. Proceedings of the 15th International Technical Meeting of the Satellite Division of the Institute of Navigation ION GPS 2002. Portland, OR, Institute of Navigation: 2799 - 2808.

[112] Teunissen, P. J. G. (1994) A new method for carrier phase ambiguity estimation. Proceedings of IEEE Plans '94, Las Vegas, NV: 862-873.

[113] Titterton, D. H. & J. L. Weston (1997) *Strapdown Inertial Navigation Technology*, Peter Peregrinus Ltd.

[114] Van Diggelen, F. (2009) *A-GPS, Assisted GPS, GNSS, and SBAS*, Artech House, Boston.

[115] Ward, P. (1996) GPS Satellite Signal Characteristics. Understanding GPS Principles and Applications. E. D. Kaplan. Boston, Artech House.

[116] Wells (1999).

[117] Wendel, J., J. Metzgar, R. Moenikes, A. Maier & G. F. Trommer (2005) A Performance Comparison of Tightly Coupled GPS/INS Navigation Systems Based on Extended and Sigma Point Kalman Filters. ION GNSS 2005, Long Beach, CA, Institute of Navigation: 456-466.

[118] Werner, W. & J. Winkel (2003) TCAR and MCAR Options With Galileo and GPS. ION GPS/GNSS 2003 Portland, OR, Institute of Navigation: 790 - 800.

[119] Wolf, R., B. Eissfeller & G. Hein (1997) A Kalman Filter for the Integration of a Low Cost INS and an Attitude GPS. International Symposium on Kinematic Systems in Geodesy, Geomatics and Navigation (KIS 1994), Banff, AB, Department of Geomatics Engineering, University of Calgary: 143-150.

[120] Yang, Y., J. A. Farrell & M. J. Barth (2000) High-Accuracy, High-Frequency Differential Carrier Phase GPS Aided Low-Cost INS. IEEE PLANS 2000, IEEE: 148-155.

[121] Yi, Y. & D. Grejner-Brzezinska (2006) Performance Comparison of the Nonlinear Bayesian Filters Supporting GPS/INS Integration. ION NTM 2006, Monterey, CA, Institute of Navigation: 977-983.

[122] Yousuf, R. (2005) *Evaluation and Enhancement of the Wide Area Augmentation System*, MSc Thesis, Geomatics Engineering, University of Calgary, Calgary

[123] Zhang, J. H. (1999) *Investigations into the Estimation of Residual Tropospheric Delays in a GPS Network*, MSc Thesis, Department of Geomatics Engineering, University of Calgary, Calgary

[124] Zhang, W., M. E. Cannon, O. Julien & P. Alves (2003) Investigation of Combined GPS/GALILEO Cascading Ambiguity Resolution Schemes. Proceedings of the 16th International Technical Meeting of the Satellite Division of the Institute of Navigation ION GPS/GNSS 2003, Portland, Oregon: 2599 - 2610.

VSC-A Final Report: Appendix E-3

GPS Service Availability Study Final Report

Prepared by

PLAN Group
University of Calgary

List of Acronyms

AT	Along Track (component of the IVV)
CAMP	Crash Avoidance Metrics Partnership
CICAS-V	Cooperative Intersection Collision Avoidance System – Violation
CCIT	Calgary Center for Innovative Technology
CD	Cumulative Distribution
CDF	Cumulative Distribution Function
DOP	Dilution of Precision as HDOP, VDOP, PDOP, TDOP, GDOP (Horizontal, Vertical, Position, Time, Geometric)
DPOS	Difference in Position
DSRC	Dedicated Short Range Communications
ECEF	Earth Centered Earth Fixed
ENU	East North Up (Local Frame)
FHWA	Federal Highway Administration
GDOP	Geometric Dilution of Precision
GLONASS	Global Navigation Satellite System
GNSS	Global Navigation Satellite System
GPS	Global Positioning System
HW	Hardware
INS	Inertial Navigation System
ITS	Intelligent Transportation Systems
IVV	Inter-Vehicle Vector
NHTSA	National Highway Traffic Safety Administration
RAIM	Receiver Autonomous Integrity Monitoring
RMS	Root Mean Squared
RTK	Real-Time Kinematic
SP	Single Point
SW	Software
USDOT	United States Department of Transportation
VSC2	Vehicle Safety Communications 2
VSC-A	Vehicle Safety Communications – Applications

V2V	Vehicle-to-Vehicle
V2I	Vehicle to Infrastructure
V2I-B	V2I where both vehicles are inside the Infrastructure zone
V2I-S	V2I where only one vehicle is inside the Infrastructure zone
WAAS	Wide Area Augmentation System
XT	Across Track (component of the IVV)

Table of Contents

List of Figures

List of Tables

1 Introduction

This study was conducted as a part of the Positioning Technology Development task of the Crash Avoidance Metrics Partnership (CAMP) Vehicle Safety Communications 2 (VSC2) consortium Vehicle Safety Communications – Applications (VSC-A) Project. A prototype positioning system was designed, developed, and evaluated as a part of the overall VSC-A Project. This study was designed to investigate the accuracy and availability of positioning information from a VSC-A-like system under various conditions and configurations.

The report is organized as follows. Sections 3 and 4 describe the data collection and processing, respectively. Section 5 introduces metrics that are used to compare the various methods of relative positioning, while Section 6 discusses measures that may be used to infer system performance in real-time. Section 7 summarizes the data that was collected, subdivided down into multiple environments. The major component of the report is Section 8 in which the results from the Vehicle-to-Vehicle (V2V) study are used to make various comparisons of the methods and receiver types utilized. In Section 9, the dependency of errors on various quantities, including the predictive measures discussed in Section 6, is analyzed. The results of the Vehicle-to-Infrastructure (V2I) tests are presented and discussed in Section 10. This is followed by conclusions and recommendations.

2 Abbreviations

2.1 Test Receivers

- AW: High quality L1 "geodetic" type receiver (uses Wide Area Augmentation System (WAAS) ranges and corrections in internal solution).
- BW: High sensitivity, "low cost" receiver (uses WAAS ranges and corrections in internal solution).
- BN: Same as BW with no WAAS use
- B24W: High sensitivity "low-cost" receiver configured to use only a limited 24 satellite constellation (first four satellites in each of the six planes) in the navigation solution. Also uses WAAS (ranging and corrections).
- B: Refers to any/all of BW, BN, and B24.

2.2 Availability Measures

Refer to Section 5.2 for the definitions of these measures.

- AWR: Availability with Certain Reference
- AWOR: Availability without Certain Reference

- FA: Full Availability
- FAWE(n): Full Availability with Error Less than n m

3 Field Test Description

This section describes the field test setup in detail, including the hardware (HW) setup and the data collected.

3.1 Vehicle Setup

Two vehicles were used for the data collection. The HW and data flow configurations for these vehicles are shown in Figure 3-1 and Figure 3-2. The equipment, as mounted on the test vehicles, is shown in Figure 3-3 and Figure 3-4.

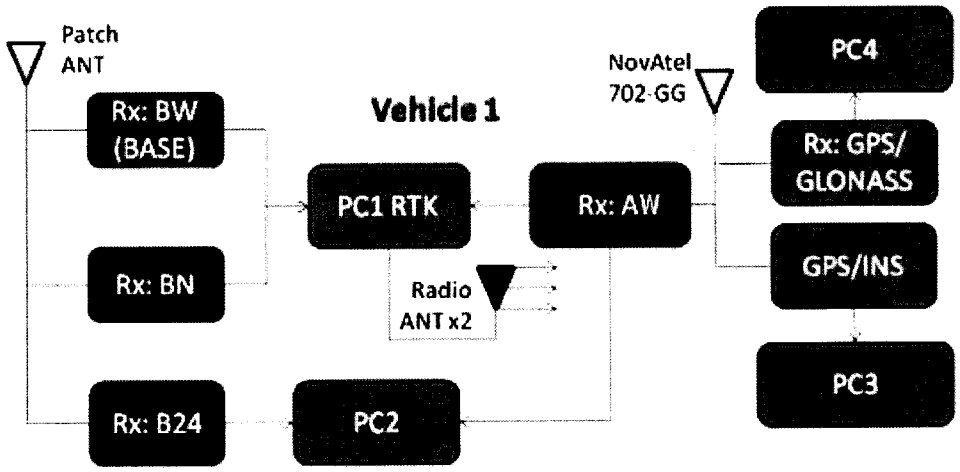

Figure 3-1: Receiver, Computer and Antenna Setup of Vehicle 1

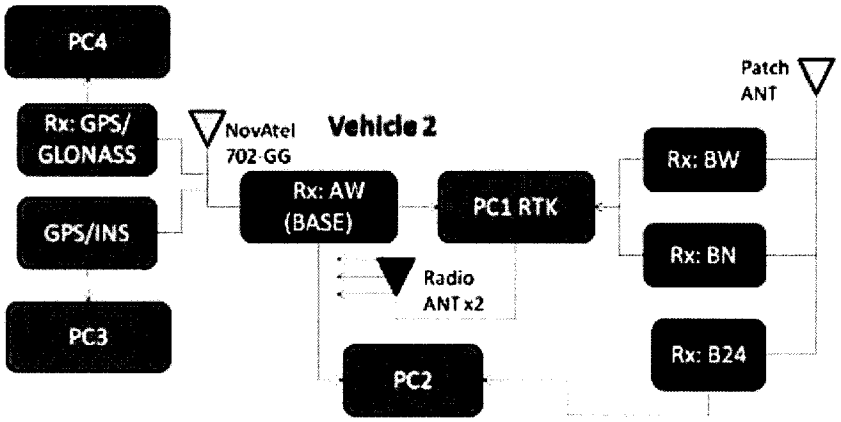

Figure 3-2: Receiver, Computer and Antenna Setup of Vehicle 2

In each vehicle, receiver AW (labeled Rx: AW in Figure 3-1 and Figure 3-2) is attached to a high quality dual-frequency Global Positioning System (GPS)+Global Navigation Satellite System (GLONASS) antenna, while receivers BW, BN, and B24W are connected to a common, low-cost patch antenna which was fixed to an aluminum plate on top of a wooden pedestal, as shown in Figure 3-4. The pedestal served the purposes of bringing the antenna to roughly the same height as the dual-frequency antenna and preventing signal shading from the equipment on the vehicle roof-racks. The aluminum plates served as ground planes for the antennas, improving their performance. The separation between the antennas on each vehicle, which was accounted for as described in Section 4, was measured to be 360 mm in each case. The antennas were positioned as closely as possible to the centerline of the vehicle.

In addition to the "test receiver," each vehicle was outfitted with additional equipment to provide reference trajectories. In particular, each vehicle had both an integrated dual frequency GPS/Inertial Navigation System (INS) system and a geodetic grade receiver configured to use both GPS and GLONASS satellites. Both systems used the aforementioned dual-frequency GPS+GLONASS antenna. The reference systems were completed with two stationary base stations located on the Calgary Center for Innovative Technology (CCIT) rooftop of the University of Calgary at precisely known WGS84 positions.

Transmission and reception of data between the two vehicles required for the Inter-Vehicle Vector (IVV) Real-Time Kinematic (RTK) calculations were achieved using Wave Radio Modules with two magnetically mounted 802.11p antennas on each vehicle for redundancy. During testing, Vehicle 1 generally followed Vehicle 2. In order to minimize the potential interference of the roof mounted instruments on the between-vehicle communications, the antennas on Vehicle 1 were located close to the front of the roof, while those on Vehicle 2 were located close to the rear of the roof. In each case, 15 cm of roof space was left to provide ground planes for the antennas.

Figure 3-3: Photograph of Test Vehicles

Figure 3-4: Equipment Setup on the Roof of Vehicle 2

3.2 V2I Setup

For the V2I data collections, the vehicle setup described in the previous section was complemented by a survey grade receiver with data logging capability attached to a

tripod mounted antenna as shown in Figure 3-5. This served the purpose of the infrastructure point required for V2I calculations.

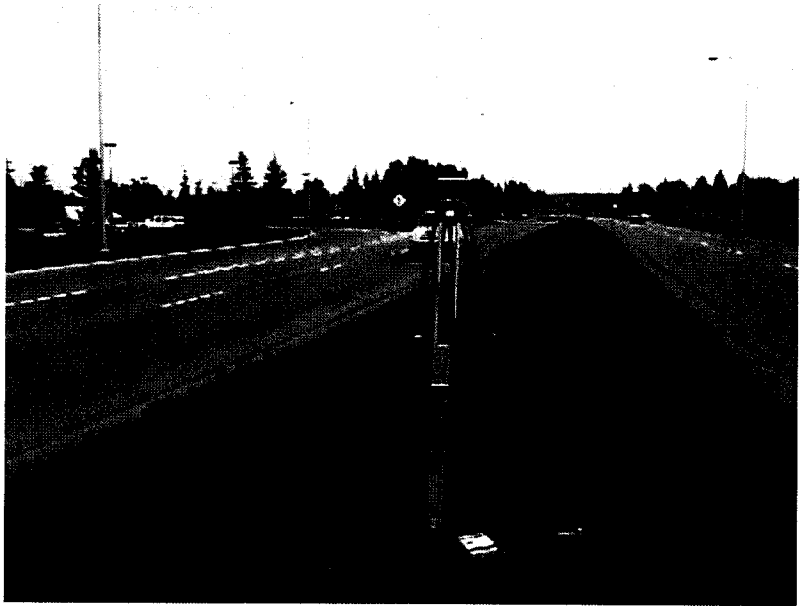

Figure 3-5: Tripod Mounted Antenna and Receiver Used in V2I Tests

3.3 Data Collected

Each of the computers, PC1 through PC4 shown in Figure 3-1 and Figure 3-2, ran specific software (SW) to facilitate calculations and data logging as follows:

- **PC1:** Commercially available RTK SW
- **PC2:** Two SW packages dedicated to AW and B type receivers
- **PC3 and PC4:** Data logging software for the reference solutions

In addition to raw measurements used for post processing, data collected by the computers on each vehicle included:

- Single Point (SP) navigation solutions for AW and B receivers: Latitude, Longitude, and Height of the relevant antenna in WGS84
- Horizontal Dilution of Precision (HDOP) and number of satellites used in the SP navigation solution for AW and B receivers
- Velocity solutions for AW and B24 receivers
- Moving base-station RTK solutions (combinations described below): Easting, Northing, and Up between the relevant antennas in units of meters

- Geometric Dilution of Precision (GDOP)[6] and number of satellites used in the moving base-station navigation solutions

All data was logged at 2 Hz. This rate was chosen as a reasonable balance between time resolution, equipment capability, and resulting data volume. As indicated in Figure 3-1 and Figure 3-2, each vehicle had a base (or host) receiver for RTK calculations. For Vehicle 1, it was BW; and for Vehicle 2, it was AW. Excluding B24W on each vehicle allowed the receiver combinations shown in Table 3-1. Thus, the RTK SW running on Vehicle 1 calculated (and logged) the moving base-station RTK solution for the AW, BW, and BN receivers on Vehicle 2 relative to the BW receiver on Vehicle 1, while the SW running on Vehicle 2 calculated and logged the solutions of the AW, BW, and BN receivers in Vehicle 1 relative to the AW receiver on Vehicle 2.

Table 3-1: RTK Combinations Processed

Vehicle 1	Vehicle 2
BW (host)	AW
	BW
	BN
AW	AW (host)
BW	
BN	

4 Data Processing

The major aim of the project was to determine the relative merits of various GPS based methods of estimating the IVV from a reference point on Vehicle 1 to a reference point on Vehicle 2 (the reference points that were used are discussed below). Thus, before describing the specific methods that were used to determine the vector, it is important to understand its definition and the frame in which it was calculated.

This IVV was obtained in one of two ways depending upon whether the method was an RTK-based method, which yields the IVV directly in terms of a local East-North-Up (ENU) frame (defined relative to the host/base), or a method based upon the absolute positions of the two vehicles, in which case the geodetic coordinates of each vehicle were transformed into the Earth-Centered-Earth-Fixed (ECEF) frame and the location of Vehicle 1 was used as the reference point to express the location of Vehicle 2 in the local ENU frame. Once obtained by one of these methods, the IVV in the ENU frame was resolved into three more physically meaningful components, namely Along Track (AT), Across Track (XT), and Up, defined relative to Vehicle 1. The first two components are generally of more interest since they position the vehicles relative to each other in the horizontal plane, as shown in Figure 4-1. During the calculations, the orientation of the Across, Along, and Up axes of Vehicle 1 was always determined using the reference GPS/INS system. Doing so ensured consistent resolution of the components for all IVV determination methods.

[6] HDOP was not available from the output of the RTK SW.